

Determination of the diffusion length and the optical self absorption coefficient using EBIC model

S. Guermazi^{1,a}, H. Guermazi¹, Y. Mlik¹, B. El Jani², C. Grill³, and A. Tourelle⁴

¹ Département de Physique, Institut Préparatoire aux Études d'Ingénieurs de Sfax, Tunisia

² Laboratoire de Physique des Matériaux, Faculté des Sciences de Monastir, Tunisia

³ Laboratoire de Microscopie Électronique, Université Montpellier 2, place Eugène Bataillon, 34000 Montpellier, France

⁴ Laboratoire d'Électrotechnique, Université Montpellier 2, place Eugène Bataillon, 34000 Montpellier, France

Received: 13 June 2000 / Revised: 30 May 2001 / Accepted: 5 June 2001

Abstract. We have developed a model of calculation of the induced current due to an electron beam. The expression for the electron beam induced current (EBIC) with an extended generation profile is obtained via the resolution of a steady state continuity equation by the Green function method, satisfying appropriated boundary conditions to the physical model. The generation profile takes into account the lateral diffusion, the effect of defects, dislocations and recombination surfaces besides the number of absorbed electrons and that of diffuse electrons as a function of the depth. In the case of a Schottky diode Au/GaAs obtained by metalorganic vapour phase epitaxy (MOVPE) method, the theoretical induced current profile is compared to the experimental one and to theoretical profiles whose analytical expressions are given by van Roosbroeck and Bresse. The minority carriers diffusion length $L_n = 2 \mu\text{m}$ and the optical self-absorption coefficient $a = 0.034 \mu\text{m}^{-1}$ can be deduced from the experimental current profile, measured by scanning electron microscopy. The theoretical curve, obtained from the proposed model is in a good agreement with the experimental one for surface recombination velocity 10^6 cm s^{-1} except for distances far from the depletion layer ($x_0 > 2.3 \mu\text{m}$) where the photocurrent produced by the multiple process of the reabsorbed recombination radiation is preponderant. Our results are in agreement with those obtained by other experimental techniques on the same samples.

PACS. 72.20.Jv Charge carriers: generation, recombination, lifetime, and trapping

1 Introduction

The diffusion length of minority carriers generated by electron beam at a plane PN junction has been determined by many authors [1–14]. They have used a focused electron beam located at varying distances from the junction.

Van Roosbroeck [1] and Bresse [2] showed that the induced current collected by a plane junction of finite thickness is given by:

$$I_{cc}(x_0) = qG_0 \frac{2}{\pi} \frac{S}{H} K_1(x_0) \quad (1)$$

where K_1 is the first order Bessel function of second kind, S is the reduced surface recombination velocity, x_0 is the reduced coordinate of a source point, H is the reduced thickness of the substrate and G_0 is the total generation rate within the generation volume. They showed that the induced current generated by an electron beam and

collected within the depletion layer for a vertical junction is of the form,

$$I_{ZC}(x_0) \propto e^{-\frac{x_0}{L}} \quad (2)$$

where x_0 is the position of the incident electron beam and L is the minority carrier diffusion length.

Berz and Kuiken [8] generalized Bresse result to arbitrary values of recombination surface velocity S . They considered van Roosbroeck and Bresse's solutions as special cases: for a point source at $Z_1 = 0$, and for surface recombination velocities $S = 0$ and $S = \infty$.

Donolato [9] has given an expression for the short circuit current for the idealized case of uniform doping and uniform density of recombination centers. He used an alternative integral representation for the induced current profile due to a point source at a finite depth, which makes use of elementary functions only. It has shown that this form is convenient both for discussing the case of an extended generation and taking into account the finite sample thickness.

^a e-mail: Samir.Guermazi@ipeis.rnu.tn

The analysis given by Oldwig Von Roos [10] has some similarities with Donolato, since he used the Fourier techniques to resolve the continuity equation with appropriate boundary conditions. He showed that the Donolato series converge much more slowly than the integral equations.

Akamatsu *et al.* [11] used the Monte Carlo method to compute the generated electron-hole pair distribution and the electron beam induced current in order to determine the minority carriers diffusion lengths. They have treated different GaAs samples: an homogeneous Schottky diode, a liquid-phase-epitaxial Schottky diode and an homostructure P-N junction with different doping levels. They have shown that the diffusion length of minority carriers is deduced from the experimental measurements near the junction for slightly doped semiconductors (transport properties), but far from the junction the measured current is produced by the multiple process of the reabsorbed recombination radiation. This additional current become also important near the junction in the case of highly doped semiconductors and for high incident electron beam accelerating voltage.

Farvacque and Sieber [12] have proposed a physical model of the EBIC contrast due to a dislocation perpendicular to the surface in the case of N-type GaAs samples. This physical approach takes into account the diffusion of minority carriers as well as the physical properties of the dislocations. The authors proved that the contribution of the recombination at the dislocation in the depletion layer to the total EBIC contrast is important either at low accelerating voltages, especially if the doping level of the semiconductor is low, or at high accelerating voltage.

Daniel *et al.* [13] have used the cathodoluminescent mode of the scanning electron microscope to deduced from experimental data the diffusion length of minority carriers, the normalized surface recombination velocity, optical absorption coefficient, dead layer thickness and a constant which combines the instrumentation constant and the quantum efficiency of radiative recombination in the case of three GaAs devices with different doping levels.

Ong *et al.* [14] have proposed a model for the calculation of the induced current due to an electron beam with an extended generation source given by:

$$I = \int_V kx^2 \frac{\lambda(x, y, z)}{g} e^{-\frac{x}{L}} dx dy dz \quad (3a)$$

where V is the generation volume, k is the proportionality constant, $\lambda(x, y, z)$ is the generation function distribution of the extended source and g is the total generation rate satisfying the relationship:

$$g = \int_V \lambda(x, y, z) dx dy dz. \quad (3b)$$

For $x > 2L$, they supposed that x is virtually constant in the integral of equation (3a) and the induced current is given by:

$$I(x) = kx^2 e^{-\frac{x}{L}}. \quad (4)$$

This method uses experimental EBIC data for the determination of bulk minority carrier diffusion length and surface recombination velocity in the case of PN junction or Schottky barrier diode. The validity of the EBIC expression is verified by the use of 3-D computer simulation.

In a previous paper [15,16], we have developed a model for the calculation of the induced current due to an electron beam with an extended generation profile in the case of a Silicon doped Au/InP Schottky diode and in the case of a sulphur doped ternary compound ($\text{Ga}_{0.7}\text{Al}_{0.3}\text{As:N}^+/\text{Ga}_{0.7}\text{Al}_{0.3}\text{As:P}$), prepared by the MOVPE method. The plane of the junction is perpendicular to the surface and the electron beam scans the surface perpendicular to the depletion layer (along the x -axis). By measuring the steady-state electron beam induced current (EBIC) as a function of the beam-junction distance, current profiles are obtained, from which the minority carrier diffusion length and the surface recombination velocity are deduced.

In this paper, a 2-D generation rate model is applied for the calculation of the collected induced current within the plane PN junction. Our results are compared with experimental ones. Then, we have focused our attention to determine the diffusion length of the excess minority carriers and the optical self-absorption coefficient of the material components generated by the electron beam from the experimental data. The surface recombination velocity is calculated from both the van Roosbroeck and Bresse model and from our proposed model, in the case of a Schottky diode Au/GaAs obtained by the MOVPE method. A comparative study between these models is then presented.

2 Theoretical study

We will investigate the case of a vertical junction silicon doped Schottky diode Au/GaAs. The incident electron beam is centred at x_0 normally to the surface. The junction is parallel to the beam (Fig. 1).

The electron beam scans the cleaved surface of the sample along the x -axis. The excess minority carrier density created within the region p is a solution of the steady-state continuity equation:

$$\nabla^2[\Delta n(x, z)] - \frac{\Delta n(x, z)}{L_n^2} = -\frac{1}{D_n}g(x, z) \quad (5)$$

that satisfies the boundary conditions associated to this physical model:

$$z = 0, \quad D_n \frac{\partial \Delta n}{\partial z} = V_S \Delta n \quad (\text{Neuman equation}) \quad (6a)$$

$$z = h, \quad D_n \frac{\partial \Delta n}{\partial z} = -V_A \Delta n \quad (\text{Neuman equation}) \quad (6b)$$

$$x = 0, \quad \Delta n = 0 \quad (\text{Dirichlet equation}) \quad (6c)$$

$$x = w_1, \quad D_n \frac{\partial \Delta n}{\partial x} = V_1 \Delta n \quad (\text{Neuman equation}) \quad (6d)$$

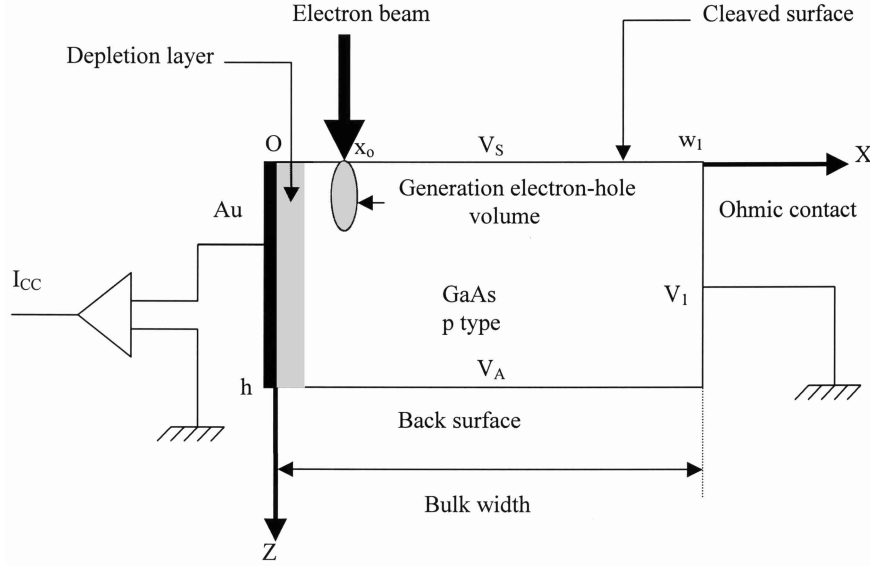


Fig. 1. Physical model.

where L_n is the diffusion length, D_n is the diffusion constant of the excess minority carriers, h is the sample thickness, V_s , V_A and V_1 are the recombination velocities respectively at the scanned surface, the back face and the ohmic contact. $g(x, z)$ is the generation rate of the excess minority carriers. Our proposed generation profile of electron-hole pairs includes the lateral diffusion taking into account the incident electron angular diffusion, the effect of defects, dislocations and surface recombination, besides the number of absorbed and diffused electrons in depth. The electron-hole pair's generation volume is an onion-shaped volume having the incident beam electron direction as a symmetry axis and containing x_0 . The generation rate depends only on the incident beam energy and the nature of the sample. Hence, the lateral diffusion is described by a Gaussian function of $(x - x_0)$ obtained by solving the equation of Bothe [17]. While, the electron diffusion in depth has a form depending on energy loss as a function of the depth proposed by Kanaya and Okayama [18]. The generation profile can be written as a convolution product of two functions [15,16]:

$$g(x - x_0, z) = \frac{(1 - \bar{R})E_0}{E_p} \frac{1}{R_K} \Phi\left(\frac{z}{R_K}\right) \frac{\alpha}{\sqrt{\pi}} e^{-\alpha^2(x-x_0)^2} \quad (7a)$$

$$R_K = \frac{AE_0^{\frac{5}{3}}}{5 \times 2^{\frac{5}{3}} \lambda_s \pi r^{\frac{1}{3}} e^{\frac{10}{3}} NZ\rho} \quad (7b)$$

where $\Phi\left(\frac{z}{R_K}\right)$ is the depth dose function and R_K is the maximum range presented by Kanaya [18]; r is the Bohr radius of the hydrogen atom; Z is the atomic number of the target; N is the Avogadro number, λ_s is a constant determined empirically [18], ρ (g cm^{-3}) is the density of the target; $A(g)$ is the atomic weight, \bar{R} is the backscattered electrons coefficient, $E_0(\text{eV})$ is the incident beam energy,

E_p (eV) is the energy gap (Eq. (7a)) and α is a parameter to be determined experimentally. For 20 keV beam incident energy, the maximum primary electron range R_K is about $4 \mu\text{m}$ in Silicon [10]. In the case of GaAs sample, the magnitude of the maximum range for $E_0 = 20 \text{ keV}$ is then $R_K = 2.3 \mu\text{m}$.

The Green function associated to equation (5) satisfying the boundary conditions (6), for an elementary source located at the point of coordinates (x', y') in the electron-hole generation volume is [10,15,16]:

$$G(x, x'; z, z') = \frac{1}{D_n} \sum_k \frac{l_k}{l_k h + \sin(l_k h)} \frac{\cos(l_k(z - \frac{h}{2})) \cos(l_k(z' - \frac{h}{2}))}{\mu_k (e^{\mu_k w_1} + K_1 e^{-\mu_k w_1})} \times \left[e^{-\mu_k(|x-x'| - w_1)} - e^{-\mu_k(x+x' - w_1)} + k_1 e^{\mu_k(x+x' - w_1)} - k_1 e^{\mu_k(|x-x'| - w_1)} \right] \quad (8)$$

where $\mu_k = \sqrt{l_k^2 + \frac{1}{L_n^2}}$, $K_1 = \frac{\mu_k - \frac{V_1}{D_n}}{\mu_k + \frac{V_1}{D_n}}$, l_k is the numerical solution of the transcendental equation $\text{tg}(l_k \frac{w_1}{2}) = \frac{V_1}{D_n} \times \frac{1}{l_k}$ deduced from (6d) boundary condition and w_1 is the right boundary limit of the sample (see Fig. 1).

The collection probability of the minority carriers generated at the point (x', z') at the junction level is defined by:

$$Q_n(x', z') = \sum_k \frac{2 \sin(l_k \frac{h}{2})}{l_k h + \sin(l_k h)} \frac{1}{e^{\mu_k w_1} + K_1 e^{-\mu_k w_1}} \times \left[e^{-\mu_k(x' - w_1)} + K_1 e^{\mu_k(x' - w_1)} \right] \times \cos\left(l_k \left(z' - \frac{h}{2}\right)\right) \quad (9)$$

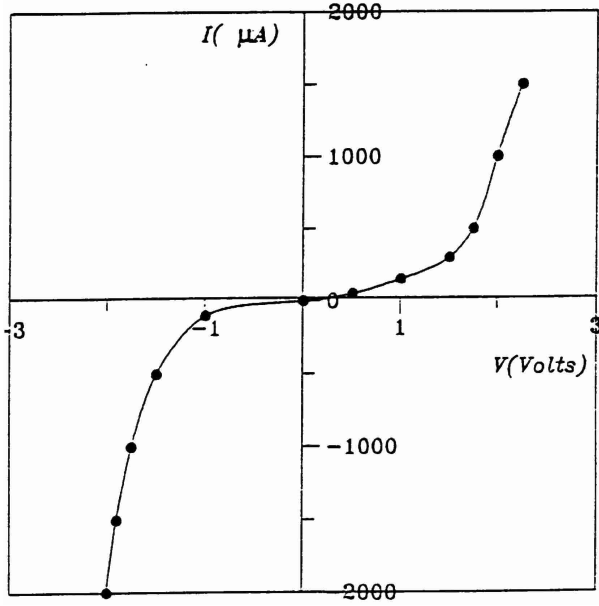


Fig. 2. Current-voltage characteristic of Au/GaAs Schottky diode.

For an extended generation, the collected current in the level of the vertical or horizontal junction is obtained from the minority carrier collection probability due to a Dirac impulse, by minority carrier generation volume integration [15,16]:

$$I_{cc} = e \iint_V Q(x', z') g(x', z') dx' dz' \quad (10)$$

where V is the generation volume. Hence, the expression of the induced current collected within the vertical junction is:

$$I_{cc} = \frac{e(1-\bar{R})E_0}{E_p} \frac{1}{R_K} \frac{\alpha}{\sqrt{\pi}} \times \sum_k \frac{2 \sin l_k \frac{h}{2}}{l_k h + \sin(l_k h)} \frac{1}{e^{\mu_k w_1} + K_1 e^{-\mu_k w_1}} \times \left[\int_0^{w_1} \left(e^{-\mu_k(x'-w_1)} + K_1 e^{\mu_k(x'-w_1)} \right) e^{-\alpha^2(x-x_0)^2} dx \right] \times \left[\int_0^{R_K} \phi \left(\frac{z'}{R_K} \right) \cos l_k \left(z' - \frac{h}{2} \right) dz' \right]. \quad (11)$$

In the case of an impulse located in the junction plane ($x = 0$), we suppose that all the carriers created within the depletion layer are collected by the junction field [20] such that the minority carriers collection probability within the depletion layer equals 1.

Then, analytical expression of the induced current generated by an electron beam and collected within the depletion layer for vertical junction is of the form [15,16]:

$$I_{ZC}(x_0) = e \iint_V g(x', z') dx' dz' \Leftrightarrow I_{ZC}(x_0) \propto e^{-\alpha^2 x_0^2} \quad (12)$$

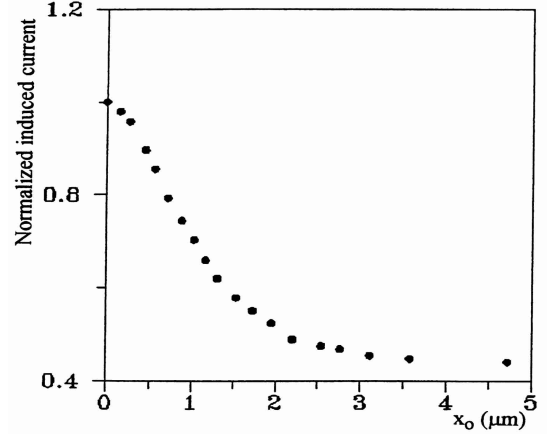


Fig. 3. Normalized induced current measured by SEMEBIC mode in Au/GaAs Schottky diode.

where V is the generation volume within the depletion layer and α , having the square root inverse of length dimension equation, is a parameter determined experimentally.

3 Experimental results

Our sample is a GaAs Schottky diode (Au/GaAs) elaborated by metalorganic vapour phase epitaxy. The MOVPE apparatus was an horizontal quartz reactor working at atmospheric pressure. During the preparation of the GaAs substrate, the doping atoms (Si) are diffused: the P doped layer was obtained by ion implantation. The sample is then submitted to a thermal annealing to ensure the activation of dopant impurities.

The P type conductivity of the sample is checked by the hot point method. An Au thin film was deposited onto the front face of the sample by evaporation under vacuum. An ohmic contact is established by annealing on the back face. An example of the current-voltage characteristics of the Au/GaAs Schottky diode is shown in Figure 2.

Our incident electron beam energy is of the order of $E_0 = 25$ keV. The circuit is indicated in Figure 1. An example of the result obtained by on line scanning is shown in Figure 3.

The shape of the normalized induced current *versus* the incident beam position decreases exponentially from a maximum at the beginning of the depletion layer.

3.1 Van Roosbroeck and Bresse model

The induced current generated by an electron beam and collected within the depletion layer for a vertical junction is of the form (2).

$$I_{ZC}(x_0) \propto e^{-\frac{x_0}{L}}. \quad (2)$$

The experimental values are shown in Figure 4 on semi logarithmic scale. The generated minority carrier diffusion

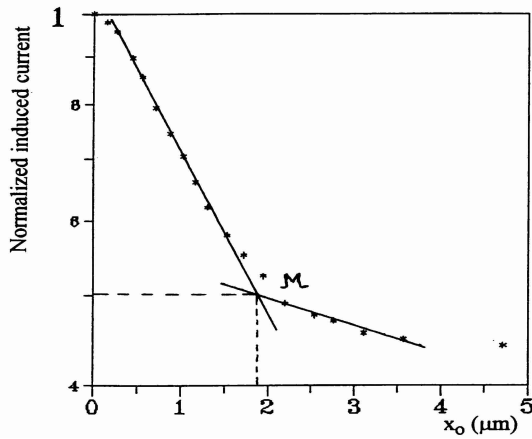


Fig. 4. Normalized induced current *versus* incident beam position on semi-logarithmic scale.

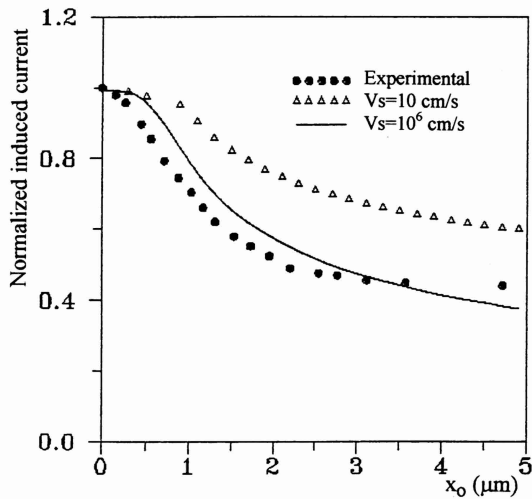


Fig. 5. Normalized induced current for $L_n = 3.5 \mu\text{m}$ and different surface recombination velocities V_s .

length is given by the inverse of the slope at the linear part (1) of the curve. Figure 4 gives $L_n = 3.5 \mu\text{m}$.

Far from the depletion layer and for the distance source-junction greater than $\frac{L_n}{2}$, we found a second linear part (2). In fact, the extrapolated linear curves cross in the point M (abscissa $1.99 \mu\text{m}$). This is due to the contribution of the multiple process of the reabsorbed, recombination, radiation (RRR) to the measured current [11–16]. The photocurrent I_{RRR} generated by the RRR process is proportional to $\exp(-ax)$, where a is a mean optical self-absorption coefficient of the sample. We found $a = 0.034 \mu\text{m}^{-1}$.

To determine the surface recombination velocity of the sample, we numerically calculated the induced current from Bresse's equation (1) [2], for many values of recombination velocity.

The obtained curves are then compared to the experimental one. All curves are shown in Figure 5. The curve corresponding to $V_s = 10^6 \text{ cm s}^{-1}$ is the most concurrent with the experimental one. We note that this curve does not coincide totally with the experimental curve at the

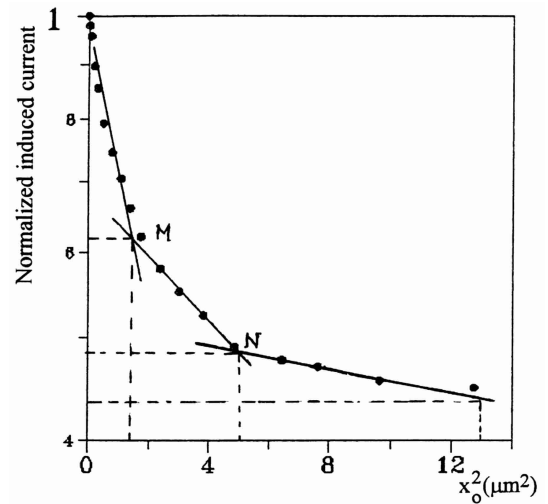


Fig. 6. Normalized induced current *versus* squared incident beam position on semi-logarithmic scale.

depletion layer and for distance source-junction greater than L_n (Fig. 5).

3.2 The proposed model

The induced current generated by an electron beam and collected within the depletion layer for a vertical junction is of the form (10) [15,16]:

$$I_{ZC}(x_0) \propto e^{-\alpha^2 x_0^2}. \quad (12)$$

The experimental values of the induced current are shown in Figure 6 on logarithmic scale as a function of x_0^2 . The curve has a decreasing exponential shape. The generated minority carrier diffusion lengths have been deduced from the inverse square root of the slope of α^2 . So, we obtain:

- from the linear part (1) of the curve, the inverse of the square root of the slope gives $L_n = 2 \mu\text{m}$;
- the linear part (2) gives $L_n = 4.5 \mu\text{m}$. This is due to the variation of the concentration in doped element.

The experimental extrapolated linear curve cross in the M position (see Fig. 6). The distance x_0^2 between origin and M is about $1.4 \mu\text{m}^2$, its square root is $x_0 = 1.18 \mu\text{m}$. This is the width of the depletion layer confirmed experimentally by the absorbed emissive mode of scanning electron microscope (see photo).

Far from the depletion layer and for distance x_0 greater than $x_N = 2.3 \mu\text{m}$, we obtain an abrupt change in the slope of the curve. This is due to the reabsorbed recombination radiation effects that are preponderant [11,15,16]. In the case of GaAs sample, a is then the optical self-absorption coefficient. This value is deduced from the square root of the slope. We obtain $a = 0.034 \mu\text{m}^{-1}$. This agrees with the value obtained by the classical model.

To determine the surface recombination velocity, we calculated numerically the induced current from our proposed model (Eq. (11)) for $L_n = 2 \mu\text{m}$ and for many values of the recombination velocity. Figure 7 shows a good

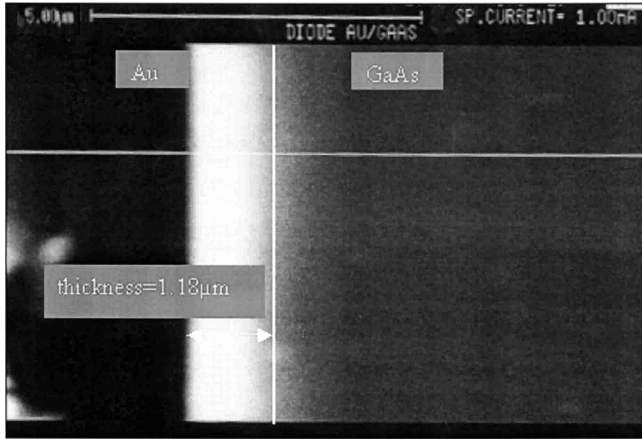


Photo : Absorbed mode of the SEM.

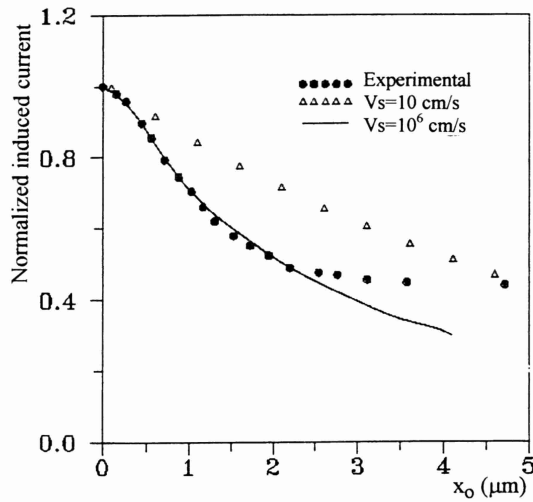


Fig. 7. Normalized induced current for $L_n = 2 \mu\text{m}$ and different surface recombination velocities V_s .

agreement of the theoretical curve ($V_s = 10^6 \text{ cm s}^{-1}$) with the experimental result in the depletion layer. We note that for distance source-junction greater than $2.3 \mu\text{m}$, the calculated curve does not coincide with the experimental one. This proves that the measured current in the region III includes the I_{RRR} current generated by the RRR process.

4 Comparative study and discussion

In order to validate our proposed EBIC model, we have carried out a comparative study with the results of the classical model [2]. By comparing the two computed curves from our model and the Bresse's one, with the measured current (Fig. 8), we notice that our calculated curve fits the experimental one within the depletion layer (region I) and in the vicinity of it (region II), unlike the curve of Bresse's model. As the source-junction distance increases (more than $2.3 \mu\text{m}$) the calculated EBIC curve diverges

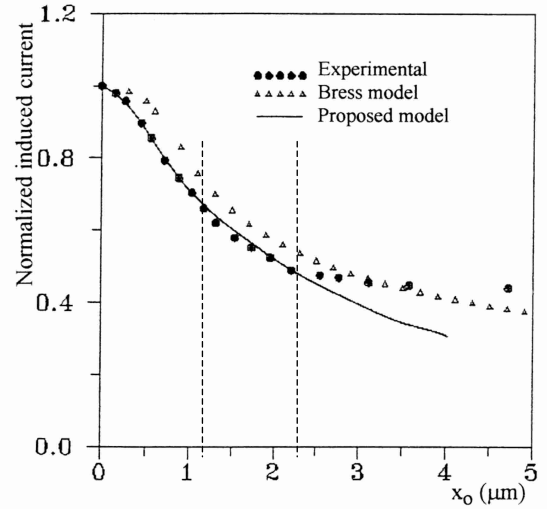


Fig. 8. Normalized induced current from different models for $V_s = 10^6 \text{ cm s}^{-1}$.

from the experimental one (in region III). This is due to the contribution of the multiple process reabsorbed recombination radiation (RRR) current which will be measured as we move away from the depletion layer. The magnitude of the normalized photocurrent generated by the RRR process is deduced by subtracting the theoretical EBIC values from the experimental values.

As the EBIC experiments have allowed us to obtain some transport properties of the component, a semi-logarithmic plot of EBIC experiments *versus* x_0^2 is achieved. From the slope of the plot we have extracted the width of the depletion layer (confirmed experimentally with absorbed mode of SEM), and the absorption coefficient.

The following table gives a comparison of measurements of diffusion length, absorption coefficient and surface recombination velocity obtained with the EBIC techniques (van Roosbroeck and Bresse model and our model) and from other measurements (Raman spectroscopy, photoluminescence intensity and Hall effect), our results are in good agreement with the experimental ones obtained by such techniques [21–23].

	L_n (μm)	a (μm^{-1})	V_s (cm s^{-1})
van Roosbroeck and Bresse model ($e^{-\frac{x_0}{L}}$)	3.5	0.034	$\approx 10^6$
Proposed model ($e^{-\frac{x_0^2}{L^2}}$)	2	0.034	10^6
Results of other experimental techniques [21–23] ^(*)	0.7–2	0.034–1	10^6

(*): Depending on minority carrier concentrations.

It is then clear that the EBIC current in the depletion layer has to be described by $e^{-\frac{x_0^2}{L^2}}$ and far from the depletion layer we have to take into account another physical process (RRR process) to fit the experimental EBIC curve.

5 Conclusion

The choice of the generation rate of the excess minority carriers generated by an electron beam is crucial to resolve the steady-state continuity equation satisfying the boundary conditions. The proposed analytical expression of the induced current within the depletion layer allowed us to determine some transport properties in III-V semiconductor materials such as the diffusion length, surface recombination velocity, as well as the width of the depletion layer. For GaAs sample, our model gives $L_n = 2 \mu\text{m}$ and $V_s = 10^6 \text{ cm s}^{-1}$. The width of the depletion layer was also deduced: $x_0 = 1.18 \mu\text{m}$.

Far from the junction the multiple process of the RRR produces most of the measured current and our model allows to deduce the optical self-absorption coefficient of the III-V semiconductor material. We found $a = 0.034 \mu\text{m}^{-1}$ for GaAs.

As the results deduced from our EBIC model are close to those obtained from several experiments (Raman spectroscopy, photoluminescence, Hall effect), we plan to apply our EBIC model to an other semiconductor devices with different doping elements and compositions for both vertical and horizontal junctions, in order to determine their transport properties.

References

1. W. van Roosbroeck, J. Appl. Phys. **26**, 380 (1955).
2. J.F. Bresse, J. Microsc. Spectrosc. Electrons **6**, 17 (1981).
3. D.B. Wittry, D.F. Kyser, J. Appl. Phys. **36**, 1387 (1965).
4. H. Higuchi, H. Tamura, Jpn. J. Appl. Phys. **4**, 316 (1965).
5. W. Czaja, J. Appl. Phys. **37**, 4236 (1966).
6. G. Lengyel, Solid-State Electron. **17**, 510 (1974).
7. H.J. Leamy, J. Appl. Phys. **53**, R51-R80 (1982).
8. F. Berz, H.K. Kuiken, Solid-State Electron. **19**, 437 (1976).
9. C. Donolato, Solid-State Electron. **25**, 1077 (1982).
10. O. Von Roos, Solid-State Electron. **21**, 1063 (1978).
11. B. Akamatsu, J. Henoc, P. Henoc, J. Appl. Phys. **52**, 7245 (1981).
12. J.L. Farvacque, B. Sieber, Rev. Phys. Appl. **25**, 353 (1990).
13. S.H. Daniel, Kin Leong Pey, Jacob C.H. Phang, IEEE Trans. Electron Devices **40**, 1417 (1993).
14. V.K.S. Ong, J.C.H. Phang, D.S.H. Chan, Solid-State Electron. **37**, 1 (1994).
15. S. Guermazi, A. Toureille, C. Grill, B. El Jani, N. Lakhoua, J. Phys. III France **6**, 481 (1996).
16. S. Guermazi, A. Toureille, C. Grill, B. El Jani, Eur. Phys. J. AP **9**, 43 (2000).
17. W. Bothe, Silzungsber Heideberger A, Kad 7, Abhandlung, 307 (1951).
18. K. Kanaya, S. Okayama, J. Phys. D Appl. Phys. **5**, 43 (1972).
19. P.H. Morse, H. Feshbach, *Methods of theoretical physics* (New York, Toronto-London, 1953), Chap. 7, Part I.
20. B. Jensen, J. Appl. Phys. **50**, 5800 (1979).
21. H.A. Zarem, P.C. Sercel, J.A. Lens, L.E. Eng, A. Yariv, K.J. Vahala, Appl. Phys. Lett. **55**, 1647 (1989).
22. R. Herlmann, G. Delgart, R. Mitdank, B. Jacobs, Phys. Stat. Sol. A **123**, 539 (1991).
23. L. Pavesi, M. Guzzi, J. Appl. Phys. **75**, 4779 (1994).